Quality Improvement Study

Medicine®

OPEN

Change in standardized uptake values in delayed ^{18}F-FDG positron emission tomography images in hepatocellular carcinoma

Kevser Oksuzoglu, MD[a], Tunc Ones, MD[a,*], Salih Ozguven, MD[a], Sabahat Inanir, MD[a], Halil Turgut Turoglu, MD[a], Emine Bozkurtlar, MD[b], Cigdem Ataizi Celikel, MD[b], Tanju Yusuf Erdil, MD[a]

Abstract

Delayed 18F-2-fluoro-2-deoxy-D-glucose (^{18}F-FDG) positron emission tomography (PET) imaging has been associated with improved diagnostic yield in several malignancies; however, data on the use of delayed imaging in patients with hepatocellular carcinoma (HCC) is scarce. This study aimed to examine tumoral and background standardized uptake value (SUV) alterations in dual-phase ^{18}F-FDG PET/computed tomography (CT) imaging.

Fifty-two HCC cases underwent dual-time-point ^{18}F-FDG PET/CT examination where early and delayed images were obtained. The maximum and mean SUVs (SUVmax and SUVmean) of the tumor were determined for both time points. Similarly, the average SUVmean were also determined for background (liver, soft tissue, and spleen). Changes in tumoral and background SUV between early and delayed images were examined.

The mean age was 62.0 ± 12.9 years (range, 20–88 years) and the majority of the patients were men (86.5%). Tumor SUVs, both tumor SUVmean and tumor SUVmax, significantly increased at delayed images when compared to early images. In contrast, the average SUVmean for the liver, soft tissue, and spleen significantly decreased at delayed images.

A significant increase in tumor SUV in delayed images in contrast to a significant decrease in background SUVs suggests that delayed images in HCC may contribute to diagnostic performance through a potential increase in the contrast between the tumor and background. However, further studies with larger sample sizes including patients with benign lesions and different grades of the disease are warranted to better elucidate the diagnostic contribution as well as the association of delayed imaging values with prognosis.

Abbreviations: ^{18}F-FDG = 18F-2-fluoro-2-deoxy-D-glucose, AASLD = American Association for the Study of Liver Diseases, HCC = hepatocellular carcinoma, PET = positron emission tomography, RECIST = Response Evaluation Criteria in Solid Tumors, ROI = regions of interest, SPSS = Statistical Package for Social Sciences, SUV = standardized uptake value.

Keywords: ^{18}F-FDG positron emission tomography, delayed images, dual-phase imaging, hepatocellular carcinoma, standardized uptake value

1. Introduction

Hepatocellular carcinoma (HCC) is the most common primary malignancy of the liver (70%–85%)[1] representing the sixth most common type of cancer and third leading cause of cancer deaths worldwide.[2] Most cases of HCC (70%–90%) develop on the grounds of chronic liver injury.

18F-2-fluoro-2-deoxy-D-glucose (^{18}F-FDG) positron emission tomography (PET) is a noninvasive imaging modality used for diagnosis, staging, restaging, and monitoring treatment response in a variety of malignancies.[3] However, its utility in patients with HCC is somewhat controversial due to differential FDG uptake depending on HCC differentiation. Well differentiated HCC display low uptake of ^{18}F-FDG, whereas poorly differentiated HCC is associated with high uptake, leading to reduced ability of ^{18}F-FDG to detect the former group of lesions and increased ability in the latter.[4–7]^{18}F-FDG PET has a sensitivity between 50% and 70% in detecting HCC.[8,9]

Previous publications have suggested that delayed imaging is associated with improved diagnostic yield as compared to standard imaging methods in a number of different malignancies including lymphoma and lung cancer.[10,11] However, literature on the use of delayed imaging in patients with HCC is scarce. Koyama et al[12] failed to detect significant contributions of delayed imaging in HCC patients. Lin et al[13] reported improved image quality with delayed imaging, and Wu et al[14] used the semiquantitative data obtained from dual-phase images to support diagnosis.

This study was undertaken to examine tumoral and background standardized uptake value (SUV) alterations in dual-phase ^{18}F-FDG PET/computed tomography (CT) imaging and to investigate the potential diagnostic contributions of dual-phase imaging in patients with HCC.

Editor: Gaurav Malhotra.

The authors have no conflicts of interest to disclose.

[a] Department of Nuclear Medicine, [b] Department of Pathology, Pendik Research and Training Hospital, Marmara University, Istanbul, Turkey.

[*] Correspondence: Tunc Ones, Department of Nuclear Medicine, Pendik Research and Training Hospital, Marmara University, Kayasultan Sokak, Aydogan Sitesi, No 58, A Blok, Daire 5, Kozyatagi/Kadikoy, Istanbul 34742, Turkey (e-mail: tones@marmara.edu.tr).

Medicine (2018) 97:42(e12817)

Received: 26 May 2018 / Accepted: 19 September 2018

http://dx.doi.org/10.1097/MD.0000000000012817

2. Methods

2.1. Patients

The study included 52 hepatocellular cancer cases that underwent dual-time-point ^{18}F-FDG PET/CT examination between February 2015 and March 2017 for their follow-up. The study protocol was approved by the institutional ethics committee (dated, January 2017; No. 09.2017.018) and written informed consent was obtained from all patients.

The diagnosis of HCC was based on histological proof in 16 patients and multidisciplinary consensus according to the noninvasive criteria of the American Association for the Study of Liver Diseases (AASLD) in 36 patients.[15] Of the 52 patients, 37 had not been treated and 15 had received transcatheter arterial embolization therapy for more than 10 weeks (ranged between 10 and 49 weeks, mean: 19.2 weeks) before the FDG PET/CT study. All tumors were >2 cm (mean tumor size: 73.35 mm; range, 20–195 mm) in diameter on CT images.

2.2. ^{18}F-FDG PET/CT imaging

All patients underwent ^{18}F-FDG PET/CT examination at the nuclear medicine department. The FDG PET/CT studies were performed using a combined PET/CT machine (Discovery-16 LS; GE Healthcare, Waukesha, WI). All patients were imaged after fasting for a minimum of 6 hours except for water and medications. All patients were required to have <200 mg/dL blood glucose level prior to injection. ^{18}F-FDG (5 MBq/kg) was injected intravenously. Whole body images from skull base to midthigh were obtained 60 ± 10 minutes after the injection (early images). Low-dose CT was performed for attenuation correction using the following parameters: 80 mA, 140 kV, and 5 mm slice thickness. PET images were obtained in 6-8 bed positions lasting 3 minutes each. The delayed imaging focusing on the liver was performed 135 ± 15 minutes after intravenous injection (delayed images) on the same scanner. PET images were reconstructed with and without correction for attenuation using an iterative algorithm then displayed for reading as sagittal, axial, and coronal views on Advantage Windows Workstation 4.5; GE Healthcare (GE Advantage, Buc, France).

2.3. Imaging data analysis

All images were examined on GE Advantage workstation by 2 experienced nuclear medicine specialists. For quantitative analysis of lesion uptake, regions of interest (ROIs) for the tumors were placed using an isocontour that included all voxels having at least 80% of the maximum radioactivity concentration. In case of no distinct tumor uptake, ROI was identified by magnetic resonance imaging or CT guidance. The maximum and mean SUVs (SUVmax and SUVmean) of the tumor were determined. ROI (circles 15 mm in diameter, 11.6 pixels) were drawn on nontumorous areas of the liver at depths of 15 and 25 mm from the liver capsule on the upper, middle, and lower third of the right lobe, respectively, at a depth of 15 mm from the liver capsule on the left lobe, and at a depth of 15 mm from the splenic capsule on 3 areas of the spleen as background. Additional soft tissue ROIs were positioned on 2 areas of the lumbar paravertebral muscle as background. The average SUVmean within background ROI was then calculated. Care was taken to avoid biliary structures and major portal, arterial, and venous vessels for background ROI. Liver, soft tissue, and spleen indexes were calculated by dividing tumor SUVmax and SUVmean by corresponding liver, soft tissue, and spleen average SUVmean for early and delayed scans. Tumor size was determined using the criteria established by the Response Evaluation Criteria in Solid Tumors (RECIST) group.[16]

Table 1

Patient demographics and clinical characteristics.

Characteristic	n = 52
Male gender	45 (86.5%)
Age, y (mean ± SD)	62.0 ± 12.0
Biopsy proven diagnosis	16 (30.8%)
Hepatitis serology	
Negative	11 (21.2%)
Hepatitis B positive	34 (65.4%)
Hepatitis C positive	7 (13.5%)
Child class	
A	36 (69.2%)
B	10 (19.2%)
C	6 (11.5%)

Unless otherwise stated, data presented in number (percentage).
SD = standard deviation.

2.4. Statistical analysis

SPSS (Statistical Package for Social Sciences) version 21 was used for the analysis of data. Data are presented in mean ± standard deviation or number (%), where appropriate. Hypothesis tests and graphical methods were used to test the normality of the distribution. For the comparison of 2 SUV at the 2 time-points, Wilcoxon signed-rank test was used. The significance of the differences between subgroups was statistically analyzed with Mann-Whitney *U* test. Spearman Correlation analysis was performed to reveal correlation between SUVs with tumor size. A *P* value <.05 was considered the indication for statistical significance.

3. Results

Fifty-two patients were included in the study. The mean age was 62.0 ± 12.9 years (range, 20–88 years) and the majority of the patients were men (86.5%). Either hepatitis B or C positivity was present in 78.9% of the patients. Table 1 summarizes demographical and clinical properties of the patients.

Tumor SUVs, both tumor SUVmean and tumor SUVmax, significantly increased at delayed images when compared to early images (Table 2). In contrast, average SUVmean for the liver, spleen, and soft tissue significantly decreased at delayed images. Table 3 shows early and delayed tumor SUVs corrected for liver, spleen, and soft tissue (i.e., indexes). In line with uncorrected tumor SUVs, all indexes for tumor SUVmax and tumor SUVmean

Table 2

SUVs at 2 time-points.

Site	Early	Delayed	*P*
Tumor SUVmax	5.8 ± 3.8	6.4 ± 4.4	<.001
Tumor SUVmean	3.4 ± 2.1	3.7 ± 2.6	<.001
Average liver SUVmean	1.9 ± 0.3	1.7 ± 0.3	<.001
Average spleen SUVmean	1.6 ± 0.3	1.5 ± 0.3	<.001
Average soft tissue SUVmean	0.6 ± 0.1	0.5 ± 0.1	.04

Data presented as mean ± standard deviation.
SUV = standardized uptake value.

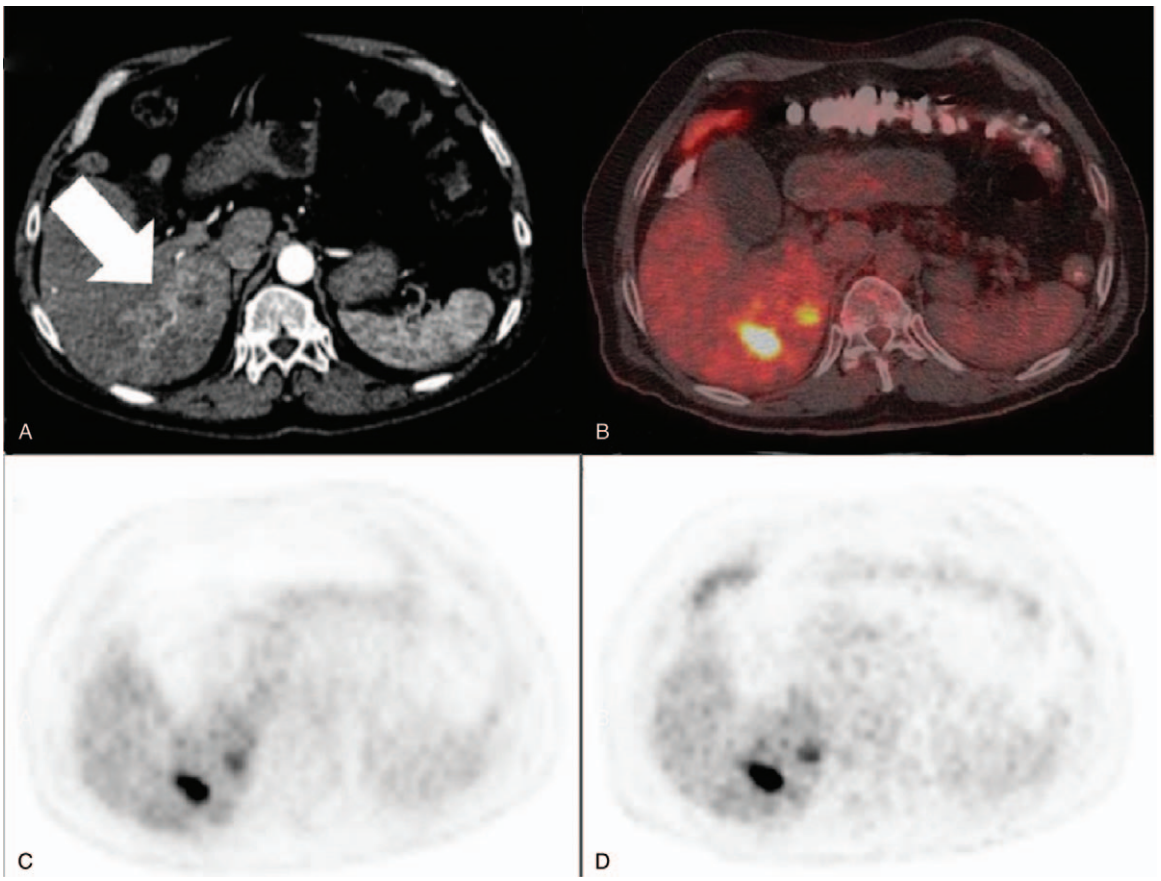

Figure 1. An example of a patient with distinct tumor uptake in which increased uptake is evident on delayed images. A, Hypervascular mass at the right lobe on contrast-enhanced computed tomography (CT). B–D, Higher tumor F-2-fluoro-2-deoxy-D-glucose (FDG) uptake at both delayed and early ^{18}F-FDG PET/CT images when compared to the liver parenchyma. Higher uptake is evident on the delayed image than the early image (SUVmax, 23.7 vs 17.8).

significantly increased at delayed images when compared to early images.

Similar relations were found when the subgroup of patients with distinct tumor uptake (n = 44) were examined, that is, increasing tumor SUVs over time in contrast to decreasing liver, soft tissue, and spleen SUVs (Fig. 1A–D). However, when small subgroup of patients without a distinct tumor uptake (n = 8) was analyzed, only significant increases in tumor SUVmax spleen index (1.8 ± 0.5 vs 1.6 ± 0.5, $P = .02$) and tumor SUVmean spleen index (1.3 ± 0.4 vs 1.1 ± 0.3, $P = .02$) and a significant decrease in average spleen SUVmean (1.4 ± 0.1 vs 1.6 ± 0.1, $P = .01$) was observed when compared to early images (Fig. 2A–D).

There was a positive correlation between tumor size and tumor SUVs in early and delayed images ($P < .001$), but no significant correlation was found between tumor size and tumor SUV changes over time (Table 4). The histopathologic grade of differentiation was high (grade I) in 7 patients, moderate (grade II) in 8 patients, and poor (grade III) in 1 patient. There was no statistical significant difference between these groups (Table 5). We were not able to compare the only one poor differentiated patient in Table 5.

According to RECIST criteria, partial regression was reported only in 6 patients and progression was seen in 8 patients and 1 patient had stable disease in the follow-up period of patients who had received transcatheter arterial embolization.[16] There were no significant differences found in SUVs and corrected tumor SUVs for liver, soft tissue, and spleen obtained at 2 time-points (i.e., early vs delayed) between the patients who had received transcatheter arterial embolization and nontreated patients (Table 6). In addition, in the subgroup of patients without distinct tumor uptake, none of them had received transcatheter arterial embolization.

4. Discussion

In the present study, a significant increase in SUV at delayed images was found in HCC lesions that exhibit higher FDG uptake than normal liver parenchyma in early images ($P < .001$). No significant correlation was found between tumor size and tumor SUV changes over time. On the basis of the number of patients/lesions assessed, this represents the second most comprehensive study in the literature examining delayed FDG uptake in HCC patients. Because of a decline in background average SUVmean as well as an increase in the contrast between the tumor and the background plane, the lesions can be more clearly visualized in delayed images. In the light of these findings, it would be more appropriate to interpret a suspicious new lesion in favor of malignancy, if there is a significant increase in SUV at delayed images in HCC patients.

Despite some studies suggesting an increased FDG uptake in lesions of malignant character, this is not a universally reported finding.[10,11,17] Nishiyama et al[18] observed higher SUVs in delayed images of tumoral lesions, whereas liver metastases could only be discerned in delayed images in 2 patients. Kubota et al[10]

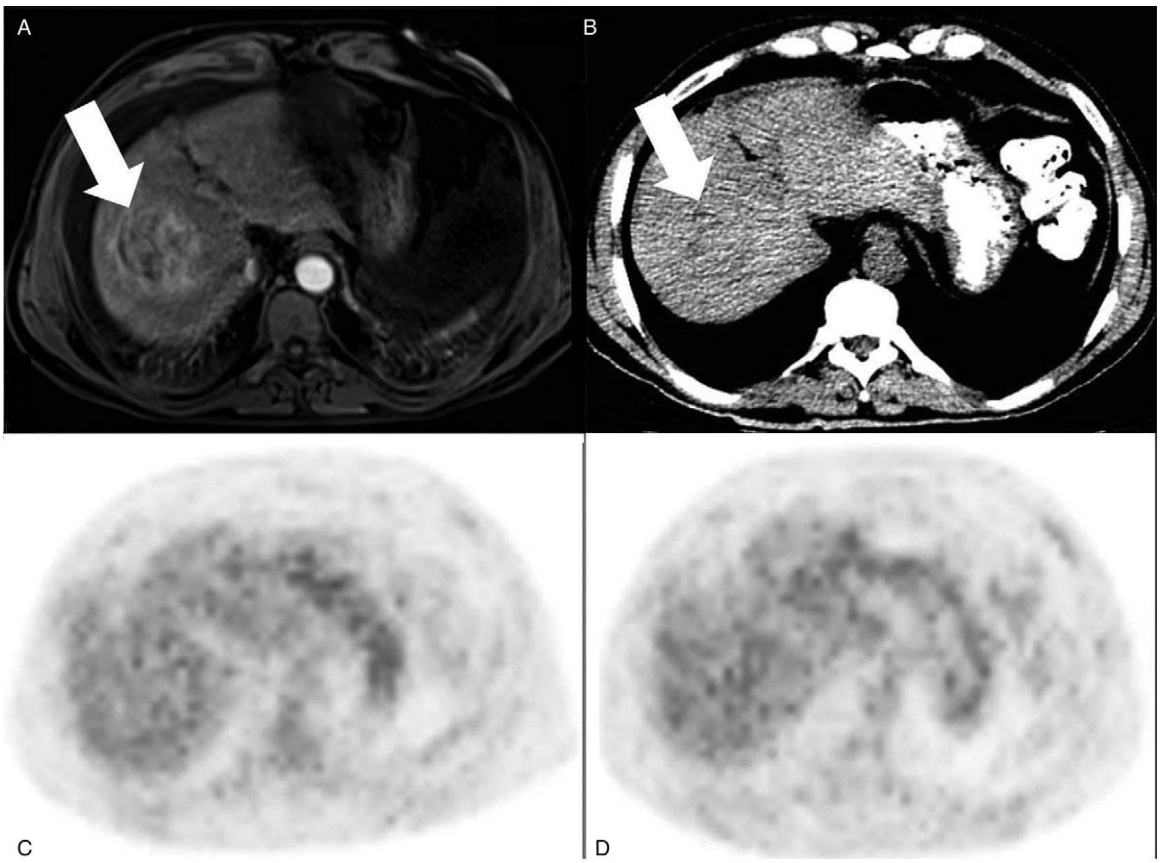

Figure 2. An example of a patient without distinct tumor uptake in which no change can be seen on delayed images. A, Hypervascular mass at the right lobe on magnetic resonance imaging (MRI). B, Hypodense mass on non–contrast-enhanced low-dose computed tomography (CT). C–D, Similar tumor 18F-2-fluoro-2-deoxy-D-glucose (FDG) uptake at both delayed and early ^{18}F-FDG PET/CT images when compared to the liver parenchyma. SUVmax 3.3 and 3.0 for early and delayed images, respectively.

found higher FDG uptake in malignant lesions in patients with lung cancer, mediastinal metastatic lymph nodes, and lymphomas, whereas bone lesions of multiple myeloma were associated with reduced FDG uptake in delayed images. Furthermore, Kubota et al detected a tendency to diminish in FDG uptake over time in the normal liver tissue, consistent with our observations. Beaulieu et al showed that in untreated locally advanced breast cancer, SUV of lesions with minimal FDG uptake are more likely to remain stable/diminish over time.[19,20] This is in line with the assertions of Cheng et al,[19] who proposed that dual-phase imaging in the differential diagnosis of pulmonary nodules with minimal affinity for FDG may be suboptimal.[21,22] Similarly, dual-phase imaging has been reported to have a limited role in characterization of lesions with no FDG affinity in patients with pancreatic cancer.[19,23]

When a consideration is given to studies of dual-phase ^{18}F-FDG PET/CT in HCC, it appears that in the study by Koyama et al[12] 9 of the total 18 HCC lesions could be detected in early images, and of the remaining 9 lesions, only 1 (1/18, 6%) could be differentiated from the normal hepatic parenchyma in delayed images. In the study by Lin et al[13] involving 16 lesions in 12 HCC patients, of the lesions that could not be separated from normal liver parenchyma in early images, only 1 (1/16, 6%)

Table 3

Tumor SUVs at the 2 time-points corrected for liver, spleen, and soft tissue.

Index	Early	Delayed	*P*
Tumor SUVmax			
Tumor SUVmax liver index	3.0±2.0	3.8±2.7	<.001
Tumor SUVmax spleen index	3.7±2.3	4.4±2.8	<.001
Tumor SUVmax soft tissue index	10.2±6.1	11.9±8.2	<.001
Tumor SUVmean			
Tumor SUVmean liver index	1.8±1.1	2.2±1.5	<.001
Tumor SUVmean spleen index	2.2±1.3	2.6±1.7	<.001
Tumor SUVmean soft tissue index	6.1±3.4	7.0±4.8	<.001

Data presented as mean±standard deviation.
SUV=standardized uptake value.

Table 4

The statistical correlation of SUVs with tumor size.

	P
Early tumor SUVmax	r=0.571 P<.001
Early tumor SUVmean	r=0.551 P<.001
Delayed tumor SUVmax	r=0.498 P<.001
Delayed tumor SUVmean	r=0.501 P<.001
Delayed—early tumor SUVmax difference	r=0.030 P=.84
Delayed—early tumor SUVmean difference	r=0.132 P=.35

Data presented as mean±standard deviation.
SUV=standardized uptake value.

Table 5

The statistical comparison of grade I HCC with grade II HCC patients.

	Grade I (n=7)	Grade II (n=8)	P
Early tumor SUVmax	3.7±1.8	4.4±2.7	.91
Early tumor SUVmean	2.2±1.0	2.7±1.5	.61
Delayed tumor SUVmax	4.2±2.1	4.7±2.8	.91
Delayed tumor SUVmean	2.3±1.1	2.8±1.6	.87

Data presented as mean±standard deviation.
HCC=hepatocellular carcinoma; SUV=standardized uptake value.

could be detected in delayed images. A comparison of our findings with those of Koyama et al and Lin et al (2/34 detected with delayed images in total; 6%), our study has failed to provide further evidence for additional diagnostic contribution of dual imaging (n=52).

In the most recent publication by Wu et al[12–14] involving 124 patients with HCC, as well as in our study, the tumor/background SUV ratio showed an increase in delayed images. Wu et al[14] are at odds with the findings reported by Lin and Koyama, reported no additional lesions that could be detected in delayed images only, and found significantly higher tumor SUVmax and tumor SUVmax/background SUVmean ratios in grade III tumors as compared to grade II tumors. In that study, tumor SUVmax of the 4 lesions which considered as grade I was reduced in delayed images. There was no statistical significant difference between grade I (n=7) and grade II (n=8) patients (Table 5) in our study. This inconsistency in the results can be due to the small number of histopathologically diagnosed cases in our study.

Table 6

The statistical comparison of the patients who had received transcatheter arterial therapy with nontreated patients.

	Treated group	Nontreated group	P
Early			
Tumor SUVmax	4.9±2.1	6.1±4.3	.66
Tumor SUVmean	2.9±1.3	3.6±2.3	.36
Average liver SUVmean	1.9±0.3	1.9±0.4	.67
Average spleen SUVmean	1.6±0.2	1.6±0.3	.81
Average soft tissue SUVmean	0.6±0.1	0.6±0.1	.43
Tumor SUVmax liver index	2.7±1.1	3.2±2.3	.97
Tumor SUVmax spleen index	3.2±1.4	3.8±2.6	.94
Tumor SUVmax soft tissue index	8.8±3.9	10.8±6.8	.40
Tumor SUVmean liver index	1.6±0.7	1.9±1.2	.68
Tumor SUVmean spleen index	1.9±0.9	2.2±1.5	.56
Tumor SUVmean soft tissue index	5.2±2.4	6.4±3.7	.17
Delayed			
Tumor SUVmax	5.7±2.1	6.7±5.1	.68
Tumor SUVmean	3.3±1.4	3.9±2.9	.90
Average liver SUVmean	1.7±0.3	1.8±0.3	.85
Average spleen SUVmean	1.4±0.2	1.5±0.3	.53
Average soft tissue SUVmean	0.6±0.1	0.5±0.1	.63
Tumor SUVmax liver index	3.4±1.4	3.9±3.1	.71
Tumor SUVmax spleen index	4.0±1.5	4.4±3.3	.52
Tumor SUVmax soft tissue index	10.5±4.1	12.5±9.3	.97
Tumor SUVmean liver index	2.0±0.9	2.3±1.7	.90
Tumor SUVmean spleen index	2.3±1.1	2.6±1.9	.82
Tumor SUVmean soft tissue index	6.0±2.7	7.3±5.4	.72

Data presented as mean±standard deviation.
SUV=standardized uptake value.

Utility of C-11 acetate in PET imaging of HCC patients has also been investigated, with high reported rates of sensitivity (87.3%) in the diagnosis well differentiated HCC.[24] Huo et al. found that dual-phase C-11 acetate PET imaging may effectively differentiate between primary HCC and focal nodular hyperplasia.[25]

^{18}F-FDG is phosphorylated to FDG-6-P after being transported into the cell by glucose carriers, and it reflects the local glucose metabolism in the cell due to its inability to proceed to glycolytic and oxidative pathways in contrast with glucose. In cells with a high content of glucose-6-phosphatase enzyme such as normal liver parenchymal cells, FDG-6-P is dephosphorylated by glucose-6-phosphatase, leading to its efflux from intracellular compartment to the extracellular compartment with a consequent and gradual decline in FDG-6-P accumulation over time.[26,27] In malignant cells, however, FDG-6-P accumulation and increased SUVs are observed due to increased hexokinase activity and decreased glucose-6-phosphatase activity. Okazumi and Torizuka,[4,28] in their multicompartment model for examining FDG transport and metabolism in HCC patients, proposed that SUVs should be measured after tumor FDG concentrations reach a plateau. Okazumi also reported differential k4 levels reflecting the activity of glucose-6-phosphatase in HCC lesions, with 45% of the HCC lesions having similar k4 content with the adjacent liver parenchyma, whereas k4 was almost zero in metastatic tumors and cholangiocellular cancers.[28] These investigators also classified HCC lesions based on the FDG uptake in the adjacent liver parenchyma as follows: type 1 lesions, high FDG uptake; type 2 lesions, comparable FDG uptake; and type 3 lesions, low FDG uptake. In type 1 lesions, elevated k3 reflecting higher hexokinase activity than the adjacent liver parenchyma as well as low k4/k3 ratios have been reported, whereas type 2 lesions had similar k4/k3 ratios and type 3 lesions had high k4/k3 ratios.[28] Torizuka et al[4] detected higher hexokinase activity and SUVs in high-grade HCC lesions than low-grade HCC lesions. Also, a predisposition for higher glucose-6-phosphatase activity in low-grade HCC was found as compared to high-grade HCC; these authors reported that ^{18}F-FDG PET results were associated with in vitro enzymatic activity of glucose and they reflect the degree of differentiation in HCC lesions.[4] Shiomi et al[29] found a correlation between tumor/background SUV ratio and tumor doubling time, with significantly lower survival in patients with a ratio exceeding 1.5. Differences in FDG uptake of patients with or without distinct tumor uptake in our study may be explained by differences in k4/k3 ratios.

The major limitation of our study is the absence of a histopathological diagnosis in a significant proportion of patients (36/52; 69%). Histopathological confirmation is not considered the criterion standard approach for a diagnosis of HCC, and we attempted to overcome this difficulty by using the typical diagnostic radiological appearance (arterial contrast enhancement, portal wash-out) as proposed by the AASLD guidelines. Another important limitation is the small number of patients (n=8) who did not exhibit significant FDG uptake both in early and delayed images. Because of the scarcity of published studies on dual-phase imaging and HCC and also due to the fact that only 2 of the patients/lesions could be discerned in delayed images rather than the early images in those studies, we believe that our findings may have a value for future studies in this field. Also, inclusion of patients with benign liver lesions in our series could have provided more clear-cut information on the diagnostic performance of dual imaging.

The heterogeneity of the cohort is another limitation of our study. The study population included both patients who had received transcatheter arterial embolization and nontreated patients. Despite this limitation, there were no significant differences between these groups (Table 6). Therefore, we can predict that the statistical results of the patients who had received trans-catheter arterial therapy did not have a statistically negative effect on the results.

5. Conclusion

In our study, a significant increase in tumor SUV and tumor/background SUV ratio was found in delayed images in HCC patients undergoing dual phase FDG PET/CT examination. Further studies with larger sample sizes including patients with benign lesions and different grades of disease are warranted to better elucidate the diagnostic contribution of this statistically significant increase in delayed images as well as the association of delayed imaging values with prognosis.

Author contributions

Conceptualization: Kevser Oksuzoglu, Tunc Ones, Salih Ozguven, Sabahat Inanir, Halil Turgut Turoglu, Emine Bozkurtlar, Cigdem Ataizi Celikel, Tanju Yusuf Erdil.
Data curation: Kevser Oksuzoglu.
Formal analysis: Tunc Ones.
Investigation: Kevser Oksuzoglu, Tunc Ones.
Methodology: Kevser Oksuzoglu, Tunc Ones.
Project administration: Tunc Ones.
Supervision: Tunc Ones, Tanju Yusuf Erdil.
Writing – original draft: Kevser Oksuzoglu, Tunc Ones.
Writing – review and editing: Tunc Ones, Salih Ozguven.
Tunc Ones orcid: 0000-0002-5992-545X.

References

[1] Jemal A, Bray F, Center MM, et al. Global cancer statistics. CA Cancer J Clin 2011;61:69–90.
[2] Forner A, Llovet JM, Bruix J. Hepatocellular carcinoma. Lancet 2012;379:1245–55.
[3] Juweid ME, Cheson BD. Positron-emission tomography and assessment of cancer therapy. N Engl J Med 2006;354:496–507.
[4] Torizuka T, Tamaki N, Inokuma T, et al. In vivo assessment of glucose metabolism in hepatocellular carcinoma with FDG-PET. J Nucl Med 1995;36:1811–7.
[5] Cho E, Jun CH, Kim BS, et al. 18F-FDG PET CT as a prognostic factor in hepatocellular carcinoma. Turk J Gastroenterol 2015;26:344–50.
[6] Li YC, Yang CS, Zhou WL, et al. Low glucose metabolism in hepatocellular carcinoma with GPC3 expression. World J Gastroenterol 2018;24:494–503.
[7] Sacks A, Peller PJ, Surasi DS, et al. Value of PET/CT in the management of primary hepatobiliary tumors, part 2. AJR Am J Roentgenol 2011; 197:W260–5.
[8] Jiang HY, Chen J, Xia CC, et al. Noninvasive imaging of hepatocellular carcinoma: from diagnosis to prognosis. World J Gastroenterol 2018; 24:2348–62.
[9] Song JY, Lee YN, Kim YS, et al. Predictability of preoperative 18F-FDG PET for histopathological differentiation and early recurrence of primary malignant intrahepatic tumors. Nucl Med Commun 2015;36:319–27.
[10] Kubota K, Itoh M, Ozaki K, et al. Advantage of delayed whole-body FDG-PET imaging for tumour detection. Eur J Nucl Med 2001;28: 696–703.
[11] Nakayama M, Okizaki A, Ishitoya S, et al. Dual-time-point F-18 FDG PET/CT imaging for differentiating the lymph nodes between malignant lymphoma and benign lesions. Ann Nucl Med 2013;27:163–9.
[12] Koyama K, Okamura T, Kawabe J, et al. The usefulness of 18F-FDG PET images obtained 2 hours after intravenous injection in liver tumor. Ann Nucl Med 2002;16:169–76.
[13] Lin WY, Tsai SC, Hung GU. Value of delayed 18F-FDG-PET imaging in the detection of hepatocellular carcinoma. Nucl Med Commun 2005;26:315–21.
[14] Wu B, Zhao Y, Zhang Y, et al. Does dual-time-point (18)F-FDG PET/CT scan add in the diagnosis of hepatocellular carcinoma? Hell J Nucl Med 2017;20:79–82.
[15] Bruix J, Sherman M. American Association for the Study of Liver Disease. Management of hepatocellular carcinoma: an update. Hepatology 2011;53:1020–2.
[16] Eisenhaur EA, Therasse P, Bogaerts J, et al. New response evaluation criteria in solid tumours: revised RECIST guideline (version 1.1). Eur J Cancer 2009;45:228–47.
[17] Yen TC, Chang YC, Chan SC, et al. Are dual-phase 18F-FDG PET scans necessary in nasopharyngeal carcinoma to assess the primary tumour and loco-regional nodes? Eur J Nucl Med Mol Imaging 2005;32:541–8.
[18] Nishiyama Y, Yamamoto Y, Fukunaga K, et al. Dual-time-point 18F-FDG PET for the evaluation of gallbladder carcinoma. J Nucl Med 2006;47:633–8.
[19] Cheng G, Torigian DA, Zhuang H, et al. When should we recommend use of dual time-point and delayed time-point imaging techniques in FDG PET? Eur J Nucl Med Mol Imaging 2013;40:779–87.
[20] Beaulieu S, Kinahan P, Tseng J, et al. SUV varies with time after injection in (18)F-FDG PET of breast cancer: characterization and method to adjust for time differences. J Nucl Med 2003;44:1044–50.
[21] Chen CJ, Lee BF, Yao WJ, et al. Dual-phase 18F-FDG PET in the diagnosis of pulmonary nodules with an initial standard uptake value less than 2.5. AJR Am J Roentgenol 2008;191:475–9.
[22] Cloran FJ, Banks KP, Song WS, et al. Limitations of dual time point PET in the assessment of lung nodules with low FDG avidity. Lung Cancer 2010;68:66–71.
[23] Higashi T, Saga T, Nakamoto Y, et al. Relationship between retention index in dual-phase (18)F-FDG PET, and hexokinase-II and glucose transporter-1 expression in pancreatic cancer. J Nucl Med 2002;43: 173–80.
[24] Ho CL, Chen S, Yeung DW, et al. Dual-tracer PET/CT imaging in evaluation of metastatic hepatocellular carcinoma. J Nucl Med 2007; 48:902–9.
[25] Huo L, Wu Z, Zhuang H, et al. Dual time point C-11 acetate PET imaging can potentially distinguish focal nodular hyperplasia from primary hepatocellular carcinoma. Clin Nucl Med 2009;34:874–7.
[26] Parghane RV, Basu S. Dual-time point 18F-FDG-PET and PET/CT for differentiating benign from malignant musculoskeletal lesions: opportunities and limitations. Semin Nucl Med 2017;47:373–91.
[27] Izuishi K, Yamamoto Y, Mori H, et al. Molecular mechanisms of [18F] fluorodeoxyglucose accumulation in liver cancer. Oncol Rep 2014;31: 701–6.
[28] Okazumi S, Isono K, Enomoto K, et al. Evaluation of liver tumors using fluorine-18-fluorodeoxyglucose PET: characterization of tumor and assessment of effect of treatment. J Nucl Med 1992;33:333–9.
[29] Shiomi S, Nishiguchi S, Ishizu H, et al. Usefulness of positron emission tomography with fluorine-18-fluorodeoxyglucose for predicting outcome in patients with hepatocellular carcinoma. Am J Gastroenterol 2001;96:1877–80.